Atmospheric Chemistry of 1,1,1-Trichloroethane: UV Spectra and Self-Reaction Kinetics of CCl3CH2 and CCl3CH2O2 Radicals, Kinetics of the Reactions of the CCl3CH2O2 Radical with NO...

ARTICLE *in* THE JOURNAL OF PHYSICAL CHEMISTRY · APRIL 1995

Impact Factor: 2.78 · DOI: 10.1021/j100017a044

4 AUTHORS, INCLUDING:

Ole John Nielsen
University of Copenhagen
261 PUBLICATIONS **4,881** CITATIONS

SEE PROFILE

Atmospheric Chemistry of 1,1,1-Trichloroethane: UV Absorption Spectra and Self-Reaction Kinetics of CCl_3CH_2 and $CCl_3CH_2O_2$ Radicals, Kinetics of the Reactions of the $CCl_3CH_2O_2$ Radical with NO and NO_2, and the Fate of the Alkoxy Radical CCl_3CH_2O

Jesper Platz, Ole J. Nielsen,* and Jens Sehested

Section for Chemical Reactivity, Environmental Science and Technology Department, Risø National Laboratory, DK-4000 Roskilde, Denmark

Timothy J. Wallington*

Ford Research Laboratory, SRL-3083, Ford Motor Company, Dearborn, P.O. Box 2053, Michigan 48121-2053

Received: October 25, 1994; In Final Form: February 10, 1995[⊗]

A pulse radiolysis technique was used to measure the UV absorption spectra of CCl_3CH_2 and $CCl_3CH_2O_2$ radicals over the range 220−300 nm. At 220 nm, $\sigma(CCl_3CH_2) = (9.4 \pm 1.1) \times 10^{-18}$ cm^2 molecule^{-1}; at 250 nm, $\sigma(CCl_3CH_2O_2) = (2.9 \pm 0.3) \times 10^{-18}$ cm^2 molecule^{-1}. The observed self-reaction rate constants, defined as $-d[CCl_3CH_2]/dt = 2k_4[CCl_3CH_2]$ and $-d[CCl_3CH_2O_2]/dt = 2k_{5obs}[CCl_3CH_2O_2]^2$, were $k_4 = (9.1 \pm 1.1) \times 10^{-12}$ and $k_{5obs} = (4.7 \pm 1.6) \times 10^{-12}$ cm^3 molecule^{-1} s^{-1}. The reaction of $CCl_3CH_2O_2$ radicals with NO gives CCl_2CH_2O radicals. In the atmosphere, >96% of the CCl_3CH_2O radicals react with O_2 to give CCl_3CHO. The rate constants for the reactions of $CCl_3CH_2O_2$ radicals with NO and NO_2 were determined to be $k_6 \geq 6.1 \times 10^{-12}$ cm^3 molecule^{-1} s^{-1} and $k_7 = (6.5 \pm 0.4) \times 10^{-12}$ cm^3 molecule^{-1} s^{-1}, respectively. As a part of this work, the rate constant for the reaction between F atoms and CCl_3CH_3 was determined to be $k_3 = (6.8 \pm 1.5) \times 10^{-12}$ cm^3 molecule^{-1} s^{-1}. A relative rate technique was used to measure rate constants for the reactions of Cl atoms with: CCl_3CH_3, $(9.9 \pm 2.0) \times 10^{-15}$; CCl_3CHO, $(6.0 \pm 1.3) \times 10^{-12}$; and CCl_3CH_2OH $(3.0 \pm 0.6) \times 10^{-12}$ (units of cm^3 molecule^{-1} s^{-1}) at 296 K. Results are discussed in the context of the atmospheric chemistry of 1,1,1-trichloroethane.

Introduction

By international agreement, industrial production of chlorofluorocarbons (CFCs), together with hydrochlorofluorocarbons (HCFCs), will be phased out. In 1990 there was a production of 726×10^6 kg of CCl_3CH_3, and the estimated release to the atmosphere the same year was 705×10^6 kg of CCl_3CH_3.[1] It is therefore important to establish the environmental impact of the release of CCl_3CH_3. It has been estimated that 10−15% of CCl_3CH_3 will enter the stratosphere.[2,3] In the stratosphere Cl atoms will be generated by photolysis of CCl_3CH_3. In the troposphere CCl_3CH_3 will react with OH radicals to produce alkyl radicals which will, in turn, react with O_2 to give peroxy radicals:

$$CCl_3CH_3 + OH \rightarrow CCl_3CH_2 + H_2O \quad (1)$$

$$CCl_3CH_2 + O_2 + M \rightarrow CCl_3CH_2O_2 + M \quad (2)$$

In the present work we have used pulse radiolysis to determine the UV absorption spectra of CCl_3CH_2 and $CCl_3CH_2O_2$ radicals, and the kinetics of the reactions 3−7.

$$CCl_3CH_3 + F \rightarrow CCl_3CH_2 + HF \quad (3)$$

$$CCl_3CH_2 + CCl_3CH_2 \rightarrow \text{products} \quad (4)$$

$$CCl_3CH_2O_2 + CCl_3CH_2O_2 \rightarrow \text{products} \quad (5)$$

$$CCl_3CH_2O_2 + NO \rightarrow \text{products} \quad (6)$$

$$CCl_3CH_2O_2 + NO_2 + M \rightarrow CCl_3CH_2O_2NO_2 + M \quad (7)$$

FTIR product studies were used to study the atmospheric fate of CCl_3CH_2O.

Experimental Section

Pulse Radiolysis System. The pulse radiolysis transient UV absorption setup used for the present experiments has been described in detail previously and will only be dealt with briefly here.[4] CCl_3CH_2 radicals were generated by the radiolysis of SF_6/CCl_3CH_3 gas mixtures in a 1 L stainless steel reactor with a 30 ns pulse of 2 MeV electrons from a Febetron 705B field emission accelerator. SF_6 was always in great excess and was used to generate fluorine atoms:

$$SF_6 \xrightarrow{2MeV\ e^-} F + \text{products} \quad (8)$$

$$F + CCl_3CH_3 \rightarrow CCl_3CH_2 + HF \quad (3)$$

$$CCl_3CH_2 + O_2 + M \rightarrow CCl_3CH_2O_2 + M \quad (2)$$

Four sets of experiments were performed. First, the ultraviolet absorption spectra of CCl_3CH_2 and $CCl_3CH_2O_2$ radicals were determined by observing the maximum of the transient UV absorption at short times (0−20 μs) following the pulse radiolysis of SF_6/CCl_3CH_3, and $SF_6/CCl_3CH_3/O_2$ mixtures, respectively. Second, using a longer time scale (100−400 μs), the subsequent decay of the absorption was monitored to determine the kinetics of the self-reactions 4 and 5:

* Authors to whom correspondence may be addressed.

[⊗] Abstract published in *Advance ACS Abstracts*, April 1, 1995.

0022-3654/95/2099-6570$09.00/0

$$CCl_3CH_2 + CCl_3CH_2 \rightarrow \text{products} \quad (4)$$

$$CCl_3CH_2O_2 + CCl_3CH_2O_2 \rightarrow \text{products} \quad (5)$$

Third, the rate of NO_2 formation following the pulse radiolysis of $SF_6/CCl_3CH_3/O_2/NO$ mixtures was used to measure k_6. Fourth, the rate of decay of NO_2 following the pulse radiolysis of $SF_6/CCl_3CH_3/O_2/NO_2$ mixtures was used to measure k_7.

To monitor the transient UV absorption, the output of a pulsed 150 W xenon arc lamp was multi-passed through the reaction cell using internal White type optics (40, 80, or 120 cm path length). Reagent concentrations used were: SF_6, 500−1000 mbar; O_2, 0−40 mbar; CCl_3CH_3, 0−10.0 mbar; NO, 0−1.5 mbar; and NO_2, 0−2.0 mbar. All experiments were performed at 295 K. Ultrahigh purity O_2 was supplied by L'Air Liquide, SF_6 (99.9%) was supplied by Gerling and Holz, CCl_3CH_3 (>99%) was obtained from the Fluka AG and was purified on a Al_2O_3 column, NO (>99.8%) was supplied by Messer Griesheim, and NO_2 (>98%) was supplied by Linde Technische Gase. The CCl_3CH_3 sample was degassed before use by repeated freeze−pump−thaw cycling. All other reagents were used as received.

FTIR Smog Chamber System. The FTIR system was interfaced to a 140 L pyrex reactor. Radicals were generated by the UV irradiation of mixtures of 110−890 mTorr of CCl_3CH_3, 0.1−0.6 Torr of F_2, 3.4−700 Torr of O_2 in 700 Torr total pressure with N_2 diluent at 296 K using 22 blacklamps (760 Torr = 1013 mbar). The loss of reactants and the formation of products were monitored by FTIR spectroscopy, using an analyzing path length of 27 m and a resolution of 0.25 cm^{-1}. Infrared spectra were derived from 32 co-added spectra. CCl_3CH_3, CCl_3CHO, and $COCl_2$ were monitored using their characteristic features over the wavenumber ranges 1030−1500, 950−1050 and 1740−1800, and 800−900 cm^{-1}, respectively. Reference spectra were acquired by expanding known volumes of reference materials into the reactor.

Results and Discussion

Spectrum of CCl_3CH_2 Radicals. Following the pulse radiolysis of CCl_3CH_3/SF_6 mixtures, a rapid increase in absorption in the UV (230 nm) was observed, followed by a slower decay. Figure 1A shows the transient absorption at 230 nm following the radiolysis of a mixture of 5 mbar of CCl_3CH_3, and of 995 mbar of SF_6. No absorption was observed when either 5 mbar of CCl_3CH_3 or 995 mbar of SF_6 was radiolyzed separately. We ascribe the absorption shown in Figure 1 to the formation of CCl_3CH_2 radicals and their subsequent loss by self-reaction. In this work we assume that F atoms react exclusively with CCl_3CH_3 by a H atom abstraction mechanism to give CCl_3CH_2 radicals, reaction 3. The validity of this assumption is discussed in a following section dealing with the atmospheric fate of CCl_3CH_2O radicals.

Measurement of the absolute absorption spectrum of CCl_3CH_2 radicals requires calibration of the initial F atom concentration. Additionally, experimental conditions are needed to ensure that there is 100% conversion of F atoms to CCl_3CH_2 radicals. The yield of F atoms was established by monitoring the transient absorbance at 260 nm due to methylperoxy radicals produced by radiolysis of $SF_6/CH_4/O_2$ mixtures as described previously.[5] The yield of F atoms at 1000 mbar of SF_6 was determined to be (2.8 ± 0.3) × 10^{15} molecules cm^{-3} at full irradiation dose, using a value of 3.18 × 10^{-18} cm^2 $molecule^{-1}$ for $\sigma(CH_3O_2)$ at 260 nm.[6] The quoted error on the F atom calibration includes both statistical (±2 standard deviations) and potential systematic errors associated with the 10% uncertainty in $\sigma(CH_3O_2)$. In the following, errors are propagated using conventional error analysis methods and are equal to ±2 standard deviations.

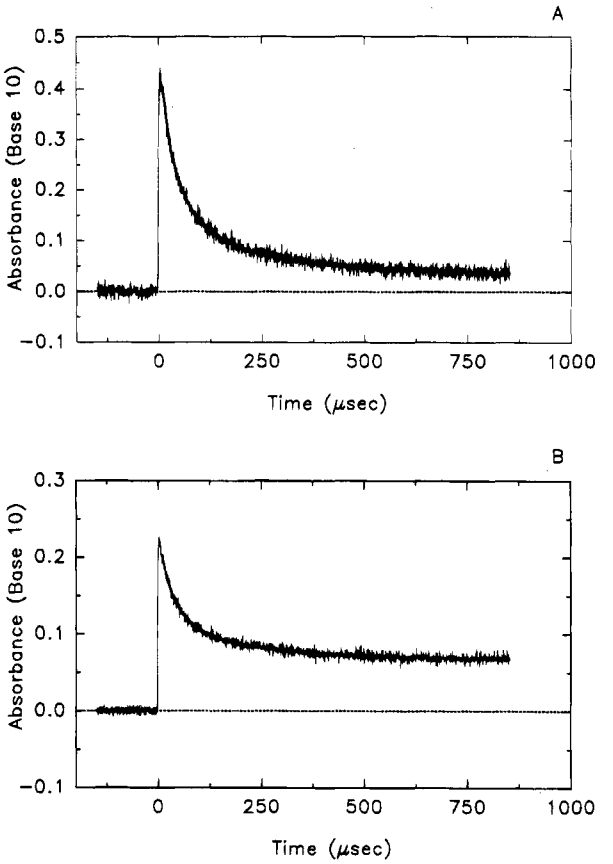

Figure 1. (A) Transient absorbance at 230 nm following the pulsed radiolysis of a mixture of 5 mbar of CCl_3CH_3 and 995 mbar of SF_6. Radiolysis dose was maximum dose; path length was 80 cm. (B) Transient absorbance at 250 nm following the pulsed radiolysis of a mixture of 10 mbar of CCl_3CH_3, 20 mbar of O_2, and 970 mbar of SF_6. Radiolysis dose was maximum dose; path length was 80 cm.

To work under conditions where the F atoms are converted stoichiometrically into CCl_3CH_2 radicals, it is necessary to consider potential interfering secondary chemistry. A complication could be reaction 9:

$$F + CCl_3CH_2 \rightarrow \text{products} \quad (9)$$

To check for complications caused by reaction 9, experiments were performed using $[CCl_3CH_3]$ = 5 mbar and $[SF_6]$ = 995 mbar in which the maximum transient absorption at 220 nm was measured as a function of the radiolysis dose. Figure 2A shows the observed maximum transient ascribed to CCl_3CH_2 radicals as a function of the dose; the optical path length was 40 cm. As shown in Figure 2A, the maximum absorption observed in experiments using high dose was significantly less than expected on the basis of a linear extrapolation of the data obtained at low dose. This observation suggests that reaction 9 is important in experiments using the maximum initial F atom concentration.

The solid line drawn through the CCl_3CH_2 data in Figure 2A is a linear least-squares fit to the low dose data and has a slope of (4.5 ± 0.3) × 10^{-1}. Combining the data with the calibrated yield of F atoms of (2.8 ± 0.3) × 10^{15} molecules cm^{-3} (full dose and $[SF_6]$ = 1000 mbar) gives $\sigma(CCl_3CH_2)$ at 220 nm = (9.4 ± 1.1) × 10^{-18} cm^2 $molecule^{-1}$. Quoted errors reflect uncertainties in both the F atom calibration and the slope of the line drawn in Figure 2A. To map out the absorption

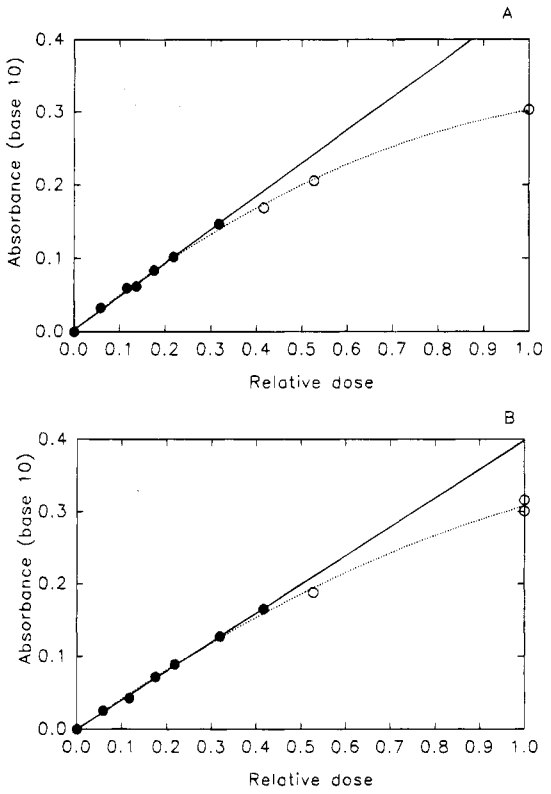

Figure 2. (A) Maximum transient absorbance at 220 nm following the pulsed radiolysis of mixtures of 5 mbar of CCl_3CH_3 and 995 mbar of SF_6 as a function of the radiolysis dose; path length was 40 cm. (B) Maximum transient absorbance at 250 nm following the pulsed radiolysis of mixtures of 10 mbar of CCl_3CH_3, 20 mbar of O_2, and 970 mbar of SF_6 as a function of the radiolysis dose; path length was 120 cm. The solid lines in A and B are linear regressions of the low dose data (filled circles). The dotted lines are second-order fits to the entire data set to aid in visual inspection of the data trend.

TABLE 1

wavelength (nm)	$\sigma(CCl_3CH_2)$ (10^{-20} cm^2 molecule^{-1})	$\sigma(CCl_3CH_2O_2)$ (10^{-20} cm^2 molecule^{-1})
220	938	327
230	648	336
240	296	348
250	169	290
260	121	213
270	77	141
280	54	81
290		44
300		25

spectrum of CCl_3CH_2 radicals, experiments were performed to measure the initial absorption between 220 and 280 nm following the pulsed irradiation of mixtures of 5 mbar of CCl_3CH_3 and 995 mbar of SF_6. Initial absorptions were then scaled to that at 220 nm and converted into absolute absorption cross sections. Values obtained are given in Table 1 and shown in Figure 3A. The spectrum is distinctly different from that of the CH_2Cl radical[7] also shown in Figure 3A.

Spectrum of $CCl_3CH_2O_2$ Radicals. Following the pulsed radiolysis of mixtures of 10 mbar of CCl_3CH_3, 20 mbar of O_2, and 970 mbar of SF_6, a rapid increase, complete within 5−10 μs, in UV absorbance in the region 220−300 nm was observed, followed by a slower decay. An example is shown in Figure 1B. We ascribe the UV absorbance resulting from radiolysis of $SF_6/CCl_3CH_3/O_2$ mixtures to $CCl_3CH_2O_2$ radicals.

To work under conditions where the F atoms are converted stoichiometrically into $CCl_3CH_2O_2$ radicals, it is necessary to consider potential interfering secondary chemistry. Potential

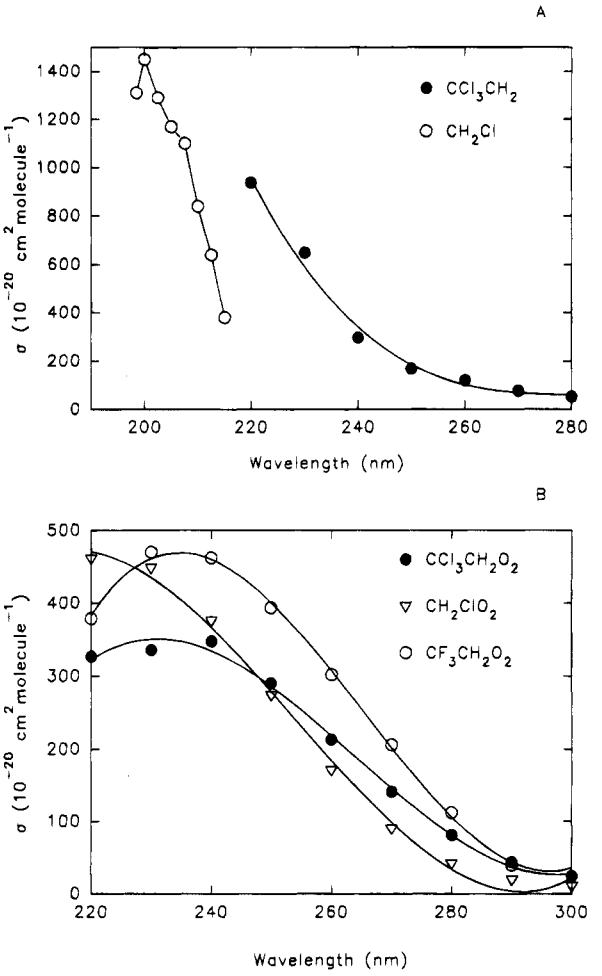

Figure 3. (A) UV-absorption spectrum of the CCl_3CH_2 radical in the range 220−280 nm. (B) UV-absorption spectrum of the $CCl_3CH_2O_2$ radical in the range 220−300 nm.

complications include: (i) loss of F atoms by reaction with molecular oxygen:

$$F + O_2 + M \rightarrow FO_2 + M \quad (10)$$

(ii) unwanted radical−radical reactions such as reaction 4, 5, 11, and 12.

$$F + CCl_3CH_2O_2 \rightarrow \text{products} \quad (11)$$

$$CCl_3CH_2 + CCl_3CH_2O_2 \rightarrow CCl_3CH_2O + CCl_3CH_2O \quad (12)$$

Using rate constants for reaction 3 and 10 measured in our laboratory, $k_3 = (6.8 \pm 1.5) \times 10^{-12}$ cm^3 molecule^{-1} s^{-1} and $k_{10} = (1.9 \pm 0.3) \times 10^{-13}$ cm^3 molecule^{-1} s^{-1},[8] we calculate that 5.5% of the F atoms are converted into FO_2 radicals and 94.5% into $CCl_3CH_2O_2$ radicals. Corrections for the presence of 5.5% of FO_2 radicals were calculated using the expression $\sigma(CCl_3CH_2O_2) = [\sigma(\text{observed}) - 0.055\sigma(FO_2)]/0.945$. Values of $\sigma(FO_2)$ are taken from the literature.[8,9]

There are no literature data concerning the kinetics of reactions 9, 11, and 12; hence we cannot calculate their importance. To check for these unwanted radical−radical reactions, the transient absorbance at 250 nm was measured in experiments using $[CCl_3CH_3] = 10$ mbar, $[O_2] = 20$ mbar, and $[SF_6] = 970$ mbar with the radiolysis dose varied over an order of magnitude. The UV path length was 120 cm. Figure 2B shows the observed maximum of the transient absorbance of $CCl_3CH_2O_2$ radicals at 250 nm as a function of dose. As seen

from Figure 2B, the maximum absorbance is linear with the radiolysis dose up to about 40% of the maximum dose. At maximum dose and half-dose, the maximum transient absorbance falls below that expected from a linear extrapolation of the low dose results. We ascribe the curvature in Figure 2B to incomplete conversion of F atoms into $CCl_3CH_2O_2$ radicals caused by secondary radical−radical reactions 9, 11, and 12 at high initial F atoms concentrations.

The solid line drawn through the data in Figure 2B is a linear least-squares fit of the low dose data. The slope is (3.98 ± 0.14) × 10^{-1}. From this value and three additional pieces of information, (i) the yield of F atoms of (2.8 ± 0.3) × 10^{15} molecule cm^{-3} (full dose and $[SF_6]$ = 1000 mbar), (ii) the conversion of F atoms into 94.5% $CCl_3CH_2O_2$ radicals and 5.5% FO_2, and (iii) the absorption cross section for FO_2 at 250 nm (σ = 1.3 × 10^{-18} cm^2 $molecule^{-1}$),[8] we derive $\sigma(CCl_3CH_2O_2)$ at 250 nm = (2.9 ± 0.3) × 10^{-18} cm^2 $molecule^{-1}$. The quoted error includes both statistical and potential systematic errors and so reflects the accuracy of the measurement.

To map out the spectrum of the $CCl_3CH_2O_2$ radical, experiments were performed to measure the initial absorbance between 220 and 300 nm following the pulsed irradiation of $SF_6/CCl_3CH_3/O_2$ mixtures. The initial absorbances were scaled to that at 250 nm and corrected for FO_2 to obtain absolute absorption cross sections. Absorption cross sections are given in Table 1 and compared to the spectra of CH_2ClO_2[9] and $CF_3CH_2O_2$[10] in Figure 3B. As seen from Figure 3B, the $CCl_3CH_2O_2$ spectrum is closely related to spectra of other halogenated peroxy radicals. The position of the maximum is consistent with the literature on peroxy radical spectra.[11] The Cl atoms on the carbon atom adjacent to the carbon bearing the O−O• group lower the absorption maximum.

Kinetic Study of the Self-Reaction of CCl_3CH_2 Radicals. Figure 1A shows a typical absorption trace obtained for the self-reaction of CCl_3CH_2 radicals, together with a nonlinear least-squares second-order decay fit. As discussed in previous publications,[12,13] the kinetic analysis of second-order decays can be complicated by the formation of products which absorb at the monitoring wavelength. This leads to a positive absorbance after all reactions have ceased. Accordingly, the experimental data were fit with a three parameter expression

$$1/B - 1/B_0 = (\ln 10)(2kt)/\sigma_{eff}L \qquad (I)$$

where $B = \log(I_\infty/I)$, $B_0 = \log(I_\infty/I')$, where I' is the minimum transmitted light intensity following the radiolysis pulse, I_∞ is the final light intensity, and I is the transmitted light at time t. k is the second-order rate constant for the self-reaction of the radicals, σ_{eff} is the absorption cross section of the radical minus that of any absorbing product formed at the monitoring wavelength (in the case of CCl_3CH_2 radical there was no observable residual absorption and $\sigma_{eff} = \sigma(CCl_3CH_2)$), and L is the monitoring UV path length (80 cm).

The decay of the transient absorption following radiolysis of CCl_3CH_3/SF_6 mixtures was monitored at a wavelength of 230 nm. The decay was well represented by this second-order least-squares fit. No residual absorption was observed, indicating the absence of any long-lived product which absorbs significantly at 230 nm. Figure 4A shows the reciprocal half-life for the decay of the absorption at 230 nm as a function of the initial absorbance due to CCl_3CH_2 radicals. A linear least-squares fit of the data in Figure 4A gives a slope of (5.7 ± 0.2) × 10^4 s^{-1} = (k_4 × 2 ln 10)/($\sigma(CCl_3CH_2)L$). The intercept of the linear regression of the data is (1.7 ± 0.6) × 10^3 s^{-1} and is significantly different from 0. This could be explained by a small amount of O_2 present in the SF_6. Using $\sigma(CCl_3CH_2)$ =

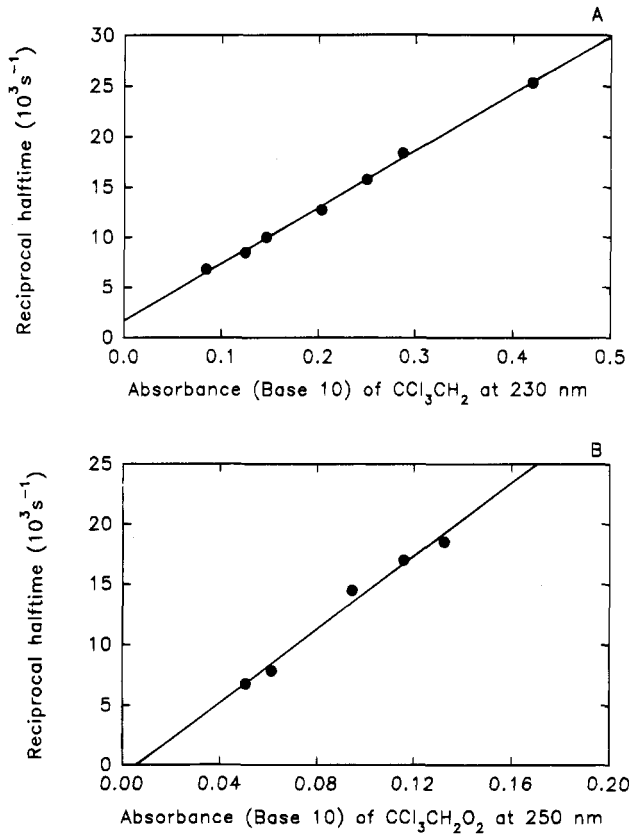

Figure 4. (A) Plot of the reciprocal half-life for the self-reaction of CCl_3CH_2 radicals as a function of A_{max} at 230 nm. (B) Plot of the reciprocal half-life for the self-reaction of $CCl_3CH_2O_2$ radicals as a function of A_{max} at 250 nm.

(9.4 ± 1.1) × 10^{-18} cm^2 $molecule^{-1}$ at 230 nm and the slope (5.7 ± 0.2) × 10^4 s^{-1}, k_4 = (9.1 ± 1.1) × 10^{-12} cm^3 $molecule^{-1}$ s^{-1} was derived. This rate constant value can be compared to typical halogenated alkyl radical self-reaction rate constants ranging from 2.4 × 10^{-12} in the case of CF_3CCl_2[14] to 3.2 × 10^{-11} cm^3 $molecule^{-1}$ s^{-1} for CH_2Cl[7] and follow the sequence $CH_2Cl > CHCl_2 > CCl_3 > CF_3CCl_2$. This order of reactivity can be rationalized in simple terms on the basis of steric arguments with bulky substituents, F and Cl atoms, slowing down the association reaction.

Kinetic Study of the Self-Reaction of the $CCl_3CH_2O_2$ Radicals. Following the pulsed radiolysis of 10 mbar of CCl_3CH_3, 20 mbar of O_2, and 970 mbar of SF_6, a rapid increase in UV absorbance in the region 220−300 nm was observed followed by a slower decay, as shown in Figure 1B. As discussed previously, we ascribe the absorbance to the $CCl_3CH_2O_2$ radicals. The decay was fit by expression I and in all cases, within the experimental uncertainties, the decays followed second-order kinetics.

The observed self-reaction rate constant of reaction 5 is defined as $-d[CCl_3CH_2O_2]/dt = 2k_{5obs}[CCl_3CH_2O_2]^2$. Figure 4B shows the reciprocal half-life for the decay of the absorption at 250 nm as a function of the initial absorbance due to $CCl_3CH_2O_2$ radicals. The absorbance is corrected for the absorption of FO_2. A linear least-squares fit of the corrected data in Figure 4B gives a slope of (9.3 ± 0.4) × 10^4 s^{-1}. The intercept of the linear regression of the data is (−3.9 ± 4.4) × 10^3 s^{-1} and is not statistically significant. Using $\sigma(CCl_3CH_2O_2)$ = (2.9 ± 0.3) × 10^{-18} cm^2 $molecule^{-1}$ at 250 nm gives k_{5obs} = (4.7 ± 1.6) × 10^{-12} cm^3 $molecule^{-1}$ s^{-1}. k_{5obs} may be an overestimate of the true bimolecular rate constant for reaction 5, as the $CCl_3CH_2O_2$ radicals might react with the reaction products, as discussed in

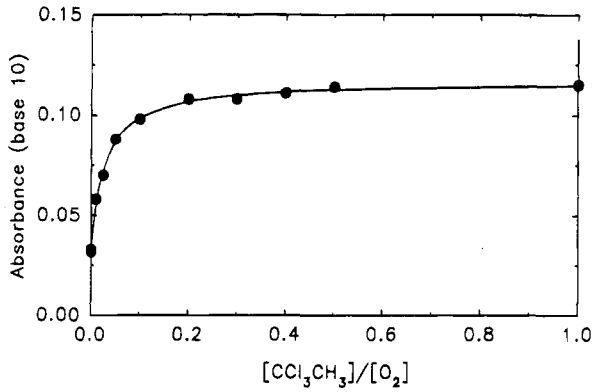

Figure 5. Plot of the maximum absorbance as a function of the concentration ratio $[CCl_3CH_3]/[O_2]$ observed following the radiolysis of $CCl_3CH_3/O_2/SF_6$ mixtures; see text for details.

ref 15. The rate constant for the self-reaction of $CCl_3CH_2O_2$ radicals is consistent with those for self-reactions of other halogenated peroxy radicals.[11] It should be pointed out that there is a large residual absorption as seen in Figure 1B. As will be discussed in the subsequent section dealing with the atmospheric fate of CCl_3CH_2O radicals, under the present experimental conditions with $[O_2] = 20$ mbar, 27% of the CCl_3CH_2O radicals formed in reaction 5 will decompose to give CCl_3 radicals which eliminate Cl atoms to give $COCl_2$. By analogy to the behavior of other peroxy radicals, $CCl_3CH_2O_2$ radicals probably react rapidly with Cl atoms to give ClO. The ClO concentration does not change on the timescale of our experiment. If all Cl atoms gave ClO, and using the recommended ClO absorption cross section at 250 nm, 3.8×10^{-18} cm^2 molecule^{-1},[16] then the residual absorption expected would be $A_{res} = 3.8 \times 10^{-18} \times 0.27 \times 2.8 \times 10^{15} \times 80 \times 0.97/2.303 = 0.097$, which compares reasonably with the observed value of 0.07. At this point it should be noted that CCl_3CHO and $COCl_2$ absorb weakly at 250 nm with absorption cross sections of 2×10^{-20} [17] and 8.1×10^{-20} cm^2 molecule^{-1},[18] respectively. The formation of CCl_3CHO and $COCl_2$ does not contribute significantly to the residual absorption seen in Figure 1B.

In light of the potential complications noted above, the value of k_{5obs} derived in the present work should be treated as an observed rate constant for the decay of absorption at 250 nm.

Reaction of F Atoms with CCl_3CH_3. To measure k_3, experiments were performed in which the maximum in the transient absorbance at 250 nm was observed following the radiolysis of $SF_6/CCl_3CH_3/O_2$ mixtures. The radiolysis dose (41.6% of full dose) and the concentration of SF_6 (980 mbar) were held fixed. The concentrations of CCl_3CH_3 and O_2 were varied over the ranges 0−20 mbar and 20−40 mbar, respectively. Figure 5 shows the observed variation of the maximum absorbance as a function of the concentration ratio $[CCl_3CH_2]/[O_2]$. In this reaction system there is a competition between 3 and 10:

$$F + CCl_3CH_3 \rightarrow CCl_3CH_2 + HF \quad (3)$$

$$F + O_2 + M \rightarrow FO_2 + M \quad (10)$$

At 250 nm, FO_2 radicals absorb less than the same amount of $CCl_3CH_2O_2$ radicals. As the CCl_3CH_3 concentration is increased, $CCl_3CH_2O_2$ radicals are formed at the expense of FO_2, and the maximum absorbance increases; see Figure 5. A_{max} increases until the ratio $[CCl_3CH_3]/[O_2]$ is about 0.2. Further increase in this ratio does not affect the maximum absorbance.

The solid line in Figure 5 is a three parameter fit of the following expression to the data:

$$A_{max} = \{A_{FO2} + A_{RO2}(k_3/k_{10})[RH]/[O_2]\}/\{1 + (k_3/k_{10})[RH]/[O_2]\}$$

where A_{max} is the observed maximum absorbance, A_{FO2} is the maximum absorbance expected if only FO_2 were produced, RH is CCl_3CH_3, and A_{RO2} is the maximum absorbance expected if only $CCl_3CH_2O_2$ were formed. Parameters A_{FO2}, A_{RO2}, and (k_3/k_{10}) were varied simultaneously. The best fit was obtained with $k_3/k_{10} = 36.0 \pm 5.3$. Using $k_{10} = (1.9 \pm 0.3) \times 10^{-13}$ cm^3 molecule^{-1} s^{-1} [8] gives $k_3 = (6.8 \pm 1.5) \times 10^{-12}$ cm^3 molecule^{-1} s^{-1}. This value is used for the calculations in this work.

Kinetic Data for the Reaction $CCl_3CH_2O_2$ + NO → Products. The kinetics of reaction 6 were studied by monitoring the increase in the absorbance at 400 nm, attributed to the formation of NO_2, following the pulsed radiolysis of $SF_6/CCl_3CH_3/O_2/NO$ mixtures. The mixtures were combinations of [NO] = 0.28−1.5 mbar, $[CCl_3CH_3] = 10$ mbar, $[O_2] = 20$ mbar, and $[SF_6] = 970$ mbar. This method of determining rates constants of reactions of peroxy radicals with NO has been used extensively in our laboratory and is discussed in detail elsewhere.[19,20] Figure 6A shows the result from a mixture with [NO] = 1.03 mbar. After the pulse radiolysis the $CCl_3CH_2O_2$ radicals will form within a few microseconds. The smooth curve in Figure 6A is a first-order fit starting 3 μs after the radiolysis pulse. The absorption transient is fitted using the expression:

$$A(t) = (A_\infty - A_0)[1 - \exp(-k^{1st}t)] + A_0 \quad (II)$$

where $A(t)$ is the absorbance as a function of time, A_∞ is the absorbance at infinite time, k^{1st} is the pseudo-first-order appearance rate of NO_2, and A_0 is the extrapolated absorbance at $t = 0$. For data shown in Figure 6A, $k^{1st} = 1.67 \times 10^5$ s^{-1}. In all cases, the rise in absorbance was well fitted by first-order kinetics. It seems reasonable to conclude that NO_2 is the species responsible for the absorbance change following pulsed radiolysis of $SF_6/CCl_3CH_3/O_2/NO$ mixtures.

As seen from Figure 7A, the pseudo-first-order rate constant, k^{1st}, increased linearly with [NO]. The initial F atom concentration employed in the present experiments (1.2×10^{15} molecule cm^{-3}) is a significant fraction (3−17%) of that of the initial NO concentration and deviations from pseudo-first-order kinetics may be expected. However, no such deviations were discernible within the experimental data scatter. Assuming that all F atoms either react directly with NO or produce species that react with NO, then the average NO concentration in a given experiment is $[NO]_{av} = [NO]_0 - [F]_0/2$. This expression was used to correct the data shown in Figure 7. Corrections applied were in the range 2−8%. Linear least-squares analysis of the data in Figure 7A gives $k_6 = (6.6 \pm 0.5) \times 10^{-12}$ cm^3 molecule^{-1} s^{-1}. The y-axis intercept in Figure 7A is $(-0.2 \pm 1.2) \times 10^4$ s^{-1} and is not statistically significant. F atom also react with NO producing FNO, $k(F + NO \rightarrow FNO) = 5.5 \times 10^{-12}$ cm^3 molecule^{-1} s^{-1}.[21] The absorption of FNO at 400 nm is negligible[22] and hence has no influence on the kinetics analysis deriving k_6.

The reaction of $CCl_3CH_2O_2$ radicals with NO produces NO_2 and, by inference, CCl_3CH_2O radicals. The alkoxy radical CCl_3CH_2O can, as discussed in a following section, react with O_2 or undergo C−C bond fission. In either case peroxy radicals (HO_2 or CCl_3O_2) will be formed which can undergo subsequent reaction with NO to give more NO_2. In the present experiments the yield of NO_2, calculated using $\sigma_{NO2}(400\text{ nm}) = 6 \times 10^{-19}$ cm^2 molecule^{-1},[31] was 162 ± 33%. The fact that the NO_2 yield exceeds 100% shows that reaction with O_2, and/or decomposition of CCl_3CH_2O radicals, takes place within our experimental

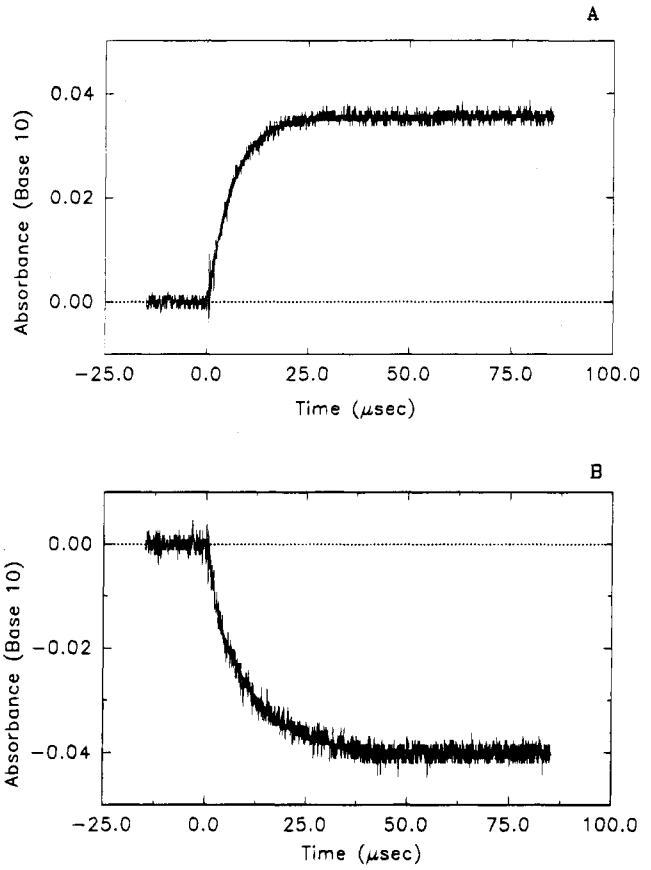

Figure 6. (A) Transient absorbance at 400 nm observed following pulsed radiolysis (dose = 42% of maximum) of a mixture of 1.03 mbar of NO, 10 mbar of CCl_3CH_3, 20 mbar of O_2, and 970 mbar of SF_6. (B) Transient absorbance at 400 nm observed following pulsed radiolysis (dose = 42% of maximum) of a mixture of 0.61 mbar of NO_2, 20 mbar of CCl_3CH_3, 20 mbar of O_2, and 960 mbar of SF_6. The path length was 120 cm in A and B.

time scale of 0−40 μs. The presence of additional processes forming NO_2 subsequent to reaction 6 increases the time taken for the NO_2 to reach a maximum, and so the value of $k_6 = (6.6 \pm 0.5) \times 10^{-12}$ cm^3 molecule^{-1} s^{-1} is actually a lower limit. Hence, we choose to give $k_6 > 6.1 \times 10^{-12}$ cm^3 molecule^{-1} s^{-1}. This value is in accordance with rate constants previously determined for RO_2 + NO reactions.[20]

Kinetic Data of the Reaction $CCl_3CH_2O_2 + NO_2 + M \rightarrow CCl_3CH_2O_2NO_2 + M$. The kinetics of reaction 7 were studied by monitoring the absorbance at 400 nm following the pulsed radiolysis of mixtures of 20 mbar of CCl_3CH_3, 20 mbar of O_2, 0.5−2.0 mbar NO_2, and SF_6 to 1000 mbar total pressure. Figure 6B shows the absorbance as a function of time after the pulsed radiolysis of a mixture with $[NO_2] = 0.61$ mbar. The absorbance before the pulsed radiolysis is due solely to the NO_2. The decay rate of the absorbance at 400 nm increased with increasing NO_2 concentration. It seems reasonable to explain the loss in absorbance by a loss of NO_2. Three reactions could be responsible:

$$F + NO_2 + M \rightarrow FNO_2/FONO + M \quad (13)$$

$$CCl_3CH_2 + NO_2 \rightarrow \text{products} \quad (14)$$

$$CCl_3CH_2O_2 + NO_2 + M \rightarrow CCl_3CH_2O_2NO_2 + M \quad (15)$$

As discussed previously,[10,23] under the present experimental conditions with $[CCl_3CH_3] = 10$ mbar and $[O_2] = 20$ mbar, reactions 13 and 14 will have a negligible influence.

The smooth curve in Figure 6B is the first-order fit of the absorption transient from 4 μs. The curve gives a pseudo-first-order rate constant k^{1st}. k^{1st} values for six experiments with different concentrations of NO_2 are shown in Figure 7B. The initial F atom concentration employed in the present experiments (1.2×10^{15} molecule cm^{-3}) is a significant fraction (2−10%) of that of the initial NO_2 concentration, and deviations from pseudo-first-order kinetics may be expected. However, no such deviations were discernible within the experimental data scatter. Assuming that all F atoms either react directly with NO_2 or produce species that react with NO_2, then the average NO_2 concentration in a given experiments is $[NO_2]_{av} = [NO_2]_0 - [F]_0/2$. This expression was used to correct the data shown in Figure 7B. Corrections applied were in the range 1−5%. Linear least-squares analysis of the data in Figure 7B gives $k_7 = (6.5 \pm 0.4) \times 10^{-12}$ cm^3 molecule^{-1} s^{-1}. The y-axis intercept in Figure 7B is $(-0.3 \pm 0.8) \times 10^4$ s^{-1} and is not statistically significant.

RO_2 + NO_2 reactions are pressure dependent and are generally at, or near, the high pressure limit at 1 atm total pressure of SF_6 diluent.[11] This value of k_7 is in accordance with rate constants previously determined for RO_2 + NO_2 reactions.[11]

Kinetics of the Reactions of Cl Atoms with CCl_3CH_3, CCl_3CHO, and CCl_3CH_2OH. Prior to investigating the atmospheric fate of CCl_3CH_2O radicals, a series of relative rate experiments was performed using the FTIR system to investigate the kinetics of the reactions of Cl atoms with CCl_3CH_3, CCl_3CHO, and CCl_3CH_2OH. The techniques used are described in detail elsewhere.[24] Photolysis of molecular chlorine was used as a source of Cl atoms.

$$Cl_2 + h\nu \rightarrow 2Cl$$

$$Cl + CCl_3CH_3 \rightarrow CCl_3CH_2 + HCl \quad (16)$$

$$Cl + CCl_3CHO \rightarrow CCl_3CO + HCl \quad (17)$$

$$Cl + CCl_3CH_2OH \rightarrow \text{products} \quad (18)$$

The kinetics of reaction 16 were measured relative to reaction 19; reactions 17 and 18 were studied relative to (20):

$$Cl + CD_4 \rightarrow CD_3 + DCl \quad (19)$$

$$Cl + C_2H_5Cl \rightarrow C_2H_4Cl + HCl \quad (20)$$

The observed losses of CCl_3CH_3 versus CD_4, CCl_3CHO versus C_2H_5Cl, and CCl_3CH_2OH versus C_2H_5Cl following the UV irradiation of $CCl_3CH_3/CD_4/Cl_2$, $CCl_3CHO/C_2H_5Cl/Cl_2$, and $CCl_3CH_2OH/C_2H_5Cl/Cl_2$ mixtures, respectively, in 700 Torr total pressure of N_2, or air, diluent are shown in Figure 8. There was no discernible difference between data obtained in N_2, or air, diluent. Linear least-squares analysis gives $k_{16}/k_{19} = (1.62 \pm 0.05)$, $k_{17}/k_{20} = 0.75 \pm 0.06$, and $k_{18}/k_{20} = 0.37 \pm 0.03$. Using $k_{19} = 6.1 \times 10^{-15}$ [24] and $k_{20} = 8.04 \times 10^{-12}$ [25] gives $k_{16} = (9.9 \pm 0.3) \times 10^{-15}$, $k_{17} = (6.0 \pm 0.5) \times 10^{-12}$, and $k_{18} = (3.0 \pm 0.2) \times 10^{-12}$ cm^3 molecule^{-1} s^{-1}, respectively. We estimate that potential systematic errors associated with uncertainties in the reference rate constants could add an additional 20% to the uncertainty range. Propagating this additional 20% uncertainty gives $k_{16} = (9.9 \pm 2.0) \times 10^{-15}$, $k_{17} = (6.0 \pm 1.3) \times 10^{-12}$, and $k_{18} = (3.0 \pm 0.6) \times 10^{-12}$ cm^3 molecule^{-1} s^{-1}.

The kinetics of reaction 16 have been studied previously by Wine et al.[26] and Tschuikow-Roux et al.[27] Using an

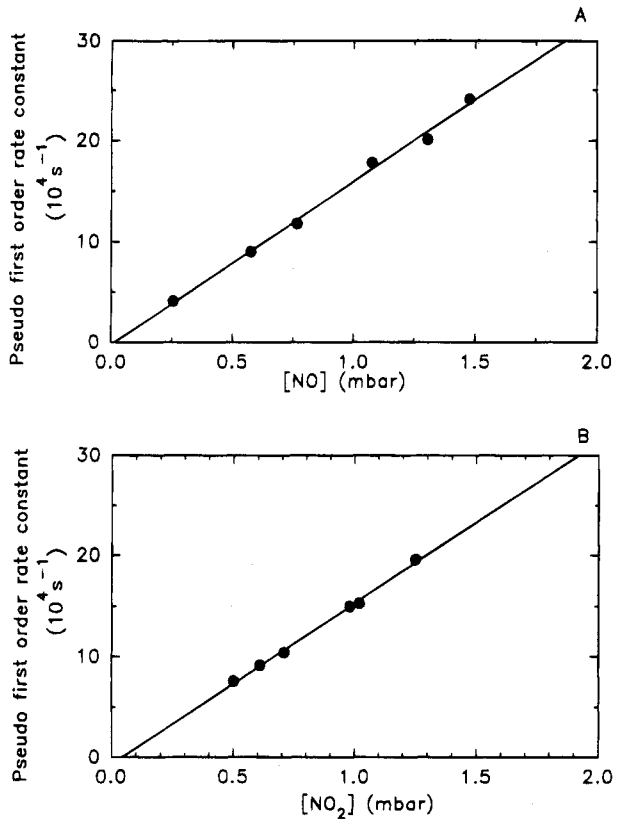

Figure 7. (A) Plot of the pseudo-first-order rate constant for the formation of NO_2 as a function of the NO concentration. (B) Plot of the pseudo-first-order rate constant for the decay of NO_2 as a function of the NO_2 concentration.

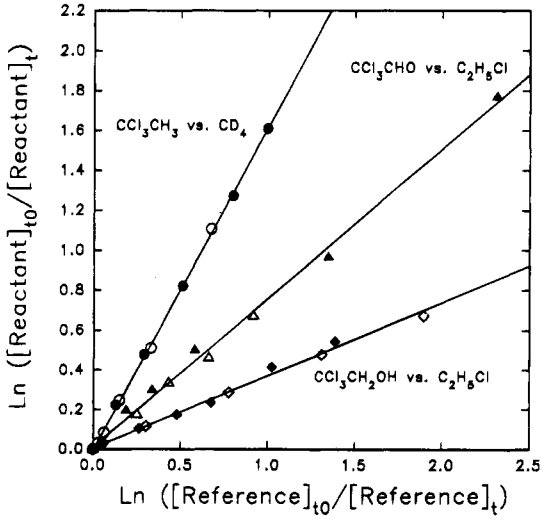

Figure 8. Results of the Cl atom relative rate experiments: observed loss of CCl_3CH_3 versus CD_4 (circles), CCl_3CHO versus C_2H_5Cl (triangles), and CCl_3CH_2OH versus C_2H_5Cl (diamonds). Filled symbols were acquired in 700 Torr of air; open symbols were acquired in 700 Torr of N_2.

absolute rate technique Wine et al.[26] measured an upper limit of $k_{16} < 3.7 \times 10^{-14}$ at room temperature while Tschuikow-Roux et al.[27] used a relative rate method to derive $k_{16} = (1.6 \pm 0.4) \times 10^{-14}$ cm^3 molecule^{-1} s^{-1}. The kinetics of reaction 17 have been studied by Scollard et al.[28] who report $k_{17} = (7.1 \pm 0.5) \times 10^{-12}$ cm^3 molecule^{-1} s^{-1}. Within the cited experimental uncertainties the results from the present work are consistent with the previous studies of k_{16} and k_{17}. There have been no studied of k_{18} with which to compare the present results.

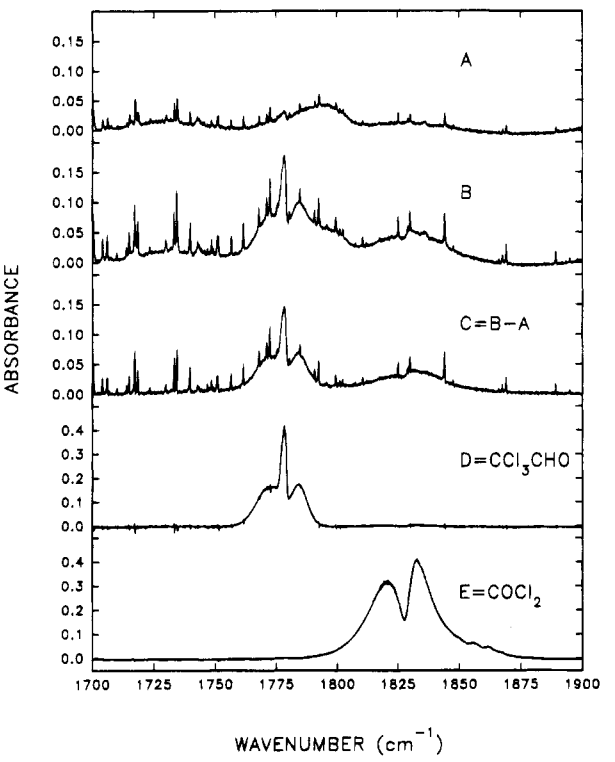

Figure 9. Infrared spectra acquired before (A) and after (B) a 1 min irradiation of a mixture of 740 mTorr of CCl_3CH_3 and 330 mTorr of F_2 in 700 Torr of air diluent (experiment 3; see Table 2). Panels D and E show reference spectra of CCl_3CHO and $COCl_2$, respectively.

Study of the Atmospheric Fate of CCl_3CH_2O Radicals. To determine the atmospheric fate of the alkoxy radical CCl_3CH_2O, experiments were performed in which $F_2/CCl_3CH_3/O_2$ mixtures at a total pressure of 700 Torr made up with N_2 diluent were irradiated in the FTIR smog chamber system. The loss of CCl_3CH_3 and the formation of products were monitored by FTIR spectroscopy. Figure 9 shows IR spectra acquired before (A) and after (B) a 1 min irradiation of a mixture of 740 mTorr of CCl_3CH_3 and 330 mTorr of F_2 in 700 Torr of air diluent (expt 3; see Table 2). Panel C (Figure 9) shows the product spectrum derived by subtracting A from B. Comparison of the product spectrum with reference spectra of CCl_3CHO and $COCl_2$ shown in panels D and E shows the formation of these products. In addition to CCl_3CHO and $COCl_2$, CO was detected as a product. Observed product yields are listed in Table 2. IR features attributable to HCHO were searched for but not found, and an upper limit of 0.1 mTorr was established for the yield of HCHO. Within the experimental errors, the observed products of CCl_3CHO and $COCl_2$ account for 100% of the loss of CCl_3CH_3. No evidence was observed for the presence of CCl_3CH_2OH in the product spectra, and an upper limit of 7% for the molar yield ($\Delta[CCl_3CH_2OH]/(\Delta[CCl_3CHO] + \Delta[COCl_2])$) of this species was established.

By analogy to the behavior of other peroxy radicals,[6,28] it is expected that the self-reaction of $CCl_3CH_2O_2$ radicals proceeds via two possible channels:

$$CCl_3CH_2O_2 + CCl_3CH_2O_2 \rightarrow CCl_3CH_2O + CCl_3CH_2O + O_2 \quad (5a)$$

$$CCl_3CH_2O_2 + CCl_3CH_2O_2 \rightarrow CCl_3CH_2OH + CCl_3CHO + O_2 \quad (5b)$$

The absence of IR features attributable to CCl_3CH_2OH product

TABLE 2: Product Yields[a] Following the Irradiation of $CCl_3CH_3/F_2/O_2$ Mixtures in 700 Torr of Diluent

exp	$[CCl_3CH_3]_0$[b]	$[F_2]_0$[b]	$[O_2]$[b]	t_{UV} (min)[c]	$\Delta[CCl_3CH_3]$	$\Delta[CCl_3CHO]$	$\Delta[COCl_2]$	$\Delta[CO]$
1	0.11	0.1	147	2	nd[d]	0.66	0.14	0.54
				4	2.2	1.09	0.84	1.33
				6	3.6	1.09	1.63	2.31
				8	4.4	1.05	3.4	3.1
				10	5.5	1.00	4.1	4.3
2	0.75	0.3	700	1	nd	1.65	0.19	0.34
3	0.74	0.3	147	1	nd	2.11	0.37	0.78
4	0.85	0.3	48	1	nd	1.45	0.56	0.54
5	0.88	0.2	17	1	nd	1.12	1.02	0.94
6	0.79	0.3	10.5	1	nd	1.32	1.11	1.08
7	0.89	0.3	10.1	1	nd	1.12	1.21	1.03
8	0.88	0.3	4.5	1	nd	0.53	1.12	1.35
9	0.88	0.6	3.4	1	nd	0.46	1.40	1.40

[a] Concentrations in units of mTorr, with no corrections of any kind applied to data. [b] Units of Torr. [c] UV lamps were not equipped with preignition coils; hence the exact irradiation times may vary. [d] Consumption of CCl_3CH_3 was not discernible.

suggests that channel 5a is dominant and channel 5b is, at most, of minor importance. This observation is consistent with the observed behavior of the analogous species CH_2ClO_2 radicals where the molecular channel of the self-reaction is of negligible (<3%) importance.[29]

CCl_3CH_2O radicals produced in reaction 5a are expected to either decompose via C−C bond scission or react with O_2:

$$CCl_3CH_2O + M \rightarrow CCl_3 + HCHO + M \quad (21)$$

$$CCl_3CH_2O + O_2 \rightarrow CCl_3CHO + HO_2 \quad (22)$$

M represents a third body such as N_2. In the presence of O_2, CCl_3 radicals undergo the following reactions leading to the formation of $COCl_2$ and Cl atoms.[30]

$$CCl_3 + O_2 + M \rightarrow CCl_3O_2 + M \quad (23)$$

$$CCl_3O_2 + RO_2\ (R = CCl_3 \text{ or } CCl_3CH_2) \rightarrow CCl_3O + RO + O_2 \quad (24)$$

$$CCl_3O + M \rightarrow COCl_2 + Cl + M \quad (25)$$

The observation of $COCl_2$ as a product following the F atom initiated oxidation of CCl_3CH_3 can be taken as an indication of the importance of reaction 21 as a fate of the alkoxy radical CCl_3CH_2O. Alternatively, $COCl_2$ may arise following unwanted secondary reactions of CCl_3CHO with either Cl or F atoms (or both) within the chamber.

$$Cl\ (F) + CCl_3CHO \rightarrow CCl_3CO + HCl\ (HF) \quad (26)$$

$$CCl_3CO + M \rightarrow CCl_3 + CO + M \quad (27)$$

Zabel et al.[31] have shown that decomposition of CCl_3CO radicals proceeds rapidly to give CO and CCl_3 radicals which will then produce $COCl_2$ and Cl atoms via reactions 23−25. The fact that the CCl_3CHO yield decreases and the $COCl_2$ yield increases with increasing conversion of CCl_3CH_3 in experiment 1 (see Table 2) shows that such secondary chemistry is important in the present work. Because Cl atoms are 600 times more reactive toward CCl_3CHO than toward CCl_3CH_3 (see previous section), loss of CCl_3CHO via reaction with Cl atoms may be important even in the presence of high CCl_3CH_3 concentrations.

The complications caused by secondary reactions involving loss of CCl_3CHO evident in the results from experiment 1 (see Table 2) render a detailed analysis of the results from this experiment difficult. However, several interesting points with regard to experiment 1 emerge from inspection of the data given in Table 2. First, after the initial 2 min irradiation period, where the impact of unwanted secondary reactions is the least, the yield of CCl_3CHO is approximately 5 times that of $COCl_2$. This observation suggests that under the experimental conditions of experiment 1 reaction 22 dominates reaction 21 as a loss of CCl_3CH_2O radicals. Second, upon further irradiation the yield of CCl_3CHO reaches a plateau whereas the $COCl_2$ yield increases markedly. This behavior is explained by the conversion of CCl_3CHO into $COCl_2$ via reactions 26, 27, 23, 24, and 25. Third, the yield of CO is similar to that of $COCl_2$ although in the early experiments the yield is substantially greater. The apparent enhanced yield of CO during the first 6 min of irradiation presumably reflects the reaction of F atoms with impurities in the chamber. Fourth, within the experimental uncertainties, the sum of the yields of CCl_3CHO and $COCl_2$ is equal to the observed loss of CCl_3CH_3, suggesting the absence of any other major products.

The observation of a significant yield of CCl_3CHO in experiment 1 suggests that reaction with O_2 is the dominant atmospheric fate of CCl_3CH_2O radicals. To quantify the relative importance of reactions 21 and 22 in the atmospheric chemistry of CCl_3CH_2O radicals, experiments 2−9 were performed in which the $[O_2]$ partial pressure was varied from 3.4 to 700 Torr. To suppress the consumption of CCl_3CHO product via Cl atom attack, high concentrations and low conversions of CCl_3CH_3 were used. The results are shown in Table 2. As seen in Table 2, as $[O_2]$ was lowered, the yield of CCl_3CHO decreased while the $COCl_2$ yield increased. The yield of CO was generally indistinguishable from that of $COCl_2$, although for experiments 2 and 3 with low yields of $COCl_2$ the CO yield somewhat larger, reflecting a small unknown source of CO in the present experiments. The observed dependence of the CCl_3CHO and $COCl_2$ yields on the partial pressure of O_2 suggests that there is a competition between reactions 21 and 22 for the available CCl_3CH_2O radicals. Ignoring for the moment the possible complications caused by secondary reactions, and assuming that CCl_3CH_2O radicals are lost solely by reactions 21 and 22, then the yields of $COCl_2$ and CCl_3CHO are related by the expression $Y(COCl_2)/Y(CCl_3CHO) = k_{21}/(k_{22}[O_2])$. Figure 10 shows a plot of $Y(COCl_2)/Y(CCl_3CHO)$ versus $1/[O_2]$. Linear least-squares analysis gives a slope $= k_{21}/k_{22} = (8.9 \pm 0.9)$ Torr.

At this point we must consider the validity of the assumptions implicit in the above derivation of the rate constant ratio k_{21}/k_{22}. By analogy to the behavior of other alkoxy radicals, two possible fates of CCl_3CH_2O radicals have been considered thus far. Recently, Jenkin et al.[32] have shown that a third possible decomposition route is available some alkoxy radicals, namely, elimination of a hydrogen atom.

$$CCl_3CH_2O + M \rightarrow CCl_3CHO + H + M \quad (28)$$

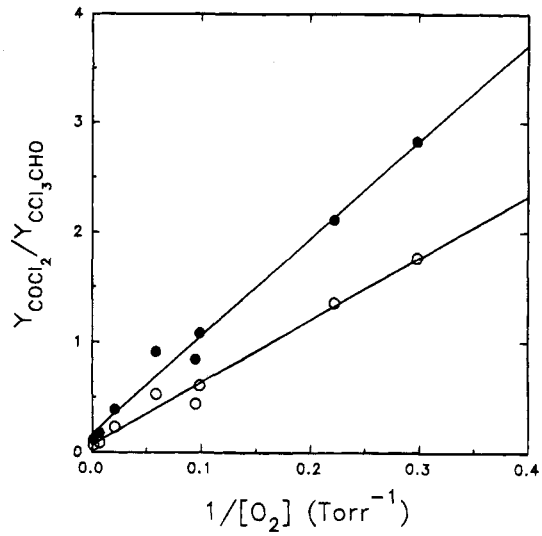

Figure 10. Plot of the ratio of the yield of $COCl_2$ to CCl_3CHO versus the reciprocal of the O_2 concentration for experiments 2−9; see Table 2 for details.

There are two factors which mitigate against reaction 28 being of importance in the present work. First, Nelson et al.[33] have estimated that reaction 28 is endothermic by 19 kcal mol^{-1}. Second, if reaction 28 were significant, no dependence of the CCl_3CHO and $COCl_2$ yields on the O_2 partial pressure would be expected. This is in marked contrast to the present experimental observations. Accordingly, it seems reasonable to assume that reaction 28 plays no significant role and that reactions 21 and 22 are the sole loss processes for CCl_3CH_2O radicals.

There is one other assumption implicit in the data analysis. This is that neither CCl_3CHO nor $COCl_2$ is lost in any secondary reactions. $COCl_2$ does not decay in the chamber either in the dark or upon irradiation with the UV fluorescent lamps. Furthermore, no loss of $COCl_2$ was observed on irradiation of mixtures of this compound with Cl_2. We conclude that $COCl_2$ is not lost via photolysis, heterogeneous reactions, or reaction with Cl atoms. Control experiments showed that CCl_3CHO is also not lost via either heterogeneous processes or photolysis. However, as shown in the previous section, CCl_3CHO does react rapidly with Cl atoms. In the chamber CCl_3CH_3, CCl_3CHO, and possibly other species compete for the available Cl atoms. The rate constant ratio $k_{17}/k_{16} = 600$ (see previous section). The concentrations of CCl_3CH_3 and CCl_3CHO in experiments 2−10 are known (see Table 2). For each $COCl_2$ molecule that is formed in the chamber one Cl atom is liberated. The observed $COCl_2$ yield provides a measure of the Cl atoms liberated in the chamber. Corrections for the loss of CCl_3CHO via reaction with Cl atoms were estimated using the following method. Let us consider experiment 2 (see Table 2) as an example of this calculation. First, the average $[CCl_3CHO]/[CCl_3CH_3]$ ratio in the experiment was $0.825/750 = 1.1 \times 10^{-3}$. The rate constant ratio $k_{17}/k_{16} = 600$ (this work). It follows that, on average, $0.66/1.66 = 40\%$ of the Cl atoms will react with CCl_3CHO while 60% will react with CCl_3CH_3. We are not concerned with those Cl atoms which react with CCl_3CH_3. The 40% of the reaction which proceeds via attack on CCl_3CHO leads to regeneration of Cl atoms which, in turn, have a 40% chance of reacting with another CCl_3CHO molecule. Hence, a chain reaction is initiated. The efficiency of the chain is given by the geometric progress $0.4 + 0.4^2 + 0.4^3 + ...$, the sum of which is $0.4/(1 - 0.4) = 0.7$. Each Cl atom generated by reaction 21 followed by (23)−(25) then leads to the loss of 0.7 molecule of CCl_3CHO and the formation of an additional 0.7 molecule of $COCl_2$. It then follows that the observed yield of $COCl_2$ is 1.7 times greater than that expected in the absence of secondary chemistry. The corrected $COCl_2$ yield is then 0.11 mTorr and the corrected CCl_3CHO yield is 1.73 mTorr. Using this approach, corrections were calculated for experiments 2−9. Corrected data are shown as the open circles in Figure 10. Linear least-squares analysis of the corrected data gives $k_{21}/k_{22} = (5.7 \pm 0.7)$ Torr.

For convenience, in the above analysis the concentration of CCl_3CHO is assumed to be constant at one-half of the experimentally observed value. This is, of course, a simplification as in reality the CCl_3CHO will increase during the experiment. To assess the magnitude of the errors introduced by making this simplification, a modelling exercise was undertaken to explicitly evaluate the impact of secondary chemistry. In this modelling exercise the Acuchem[34] chemical kinetic modelling package was used with rate constant ratios of $k_{21}/k_{22} = 5.7$ Torr and $k_{17}/k_{16} = 600$ assumed. For the initial experimental conditions given in Table 2 the simulations reproduced the observed final yields of CCl_3CHO and $COCl_2$ to within 5%, thereby supporting the data analysis methodology used above.

In computing the above corrections, we have just considered the competition between reactions 16 and 17 for the Cl atoms. In doing so we have, in effect, assumed a worse case scenario. In reality there may be other losses for Cl atoms in the chamber. For example, Cl atoms react 7300 times faster with HCHO than with CCl_3CH_3.[16] While, as noted above, HCHO was not detected as a product in the present experiments, the <0.1 mTorr upper limit for the concentration of HCHO does not preclude this species from being a significant reaction partner for Cl atoms in the present experiments. In view of the uncertainties associated with corrections needed to account for reaction of Cl atoms with CCl_3CHO, we choose to quote a final value of $k_{21}/k_{22} = (7.3 \pm 2.5)$ Torr which is an average of the corrected and uncorrected data together with error limits which encompass the extremes of the two determinations. From this rate constant ratio it can be calculated that, in the presence of 1 atm of air at 296 K, reaction with O_2 accounts for 96% of the loss of CCl_3CH_2O radicals. Reaction with O_2 dominates the fate of CCl_3CH_2O radicals at sea level. With increasing altitude in the atmosphere the temperature, total pressure, and partial pressure of O_2 all decrease. Decreasing temperature and total pressure favor reaction 22 over reaction 21 while decreasing partial pressure of O_2 will favor reaction 21 over reaction 22. Reaction 21 is a unimolecular decomposition reaction and is expected to be very sensitive to changes in temperature. Considering the conditions pertinent to the U.S. standard atmosphere over the altitude range 0−15 km[35] and neglecting the effect of total pressure, reaction 21 will slow down faster than reaction 22 if the activation energy for reaction 21 is >4 kcal mol^{-1} than that for reaction 22. By analogy with other alkoxy radicals,[36] it seems likely that the barrier to decomposition of CCl_3CH_2O radicals will be substantially greater than 4 kcal mol^{-1} larger than that for reaction with O_2, and hence it is expected that reaction with O_2 is essentially the sole atmospheric fate of CCl_3CH_2O radicals.

Finally, the results from the product study of the F atom initiated oxidation of CCl_3CH_3 can shed some light on the question of the mechanism of F atom attack. Throughout this work it has been assumed that reaction proceeds via H atom abstraction to give CCl_3CH_2 radicals. Another possibility is Cl atom abstraction to give CH_3CCl_2 radicals. In the presence of O_2, CH_3CCl_2 radicals will form peroxy radicals $CH_3CCl_2O_2$. Subsequent reactions will then either form $COCl_2$ or CH_3COCl.

As shown in Figure 10, the $COCl_2$ yield was strongly dependent on the O_2 concentration in the chamber with a yield which approached zero at high $[O_2]$. CH_3COCl was not an observed product. An upper limit of 4% for the molar yield of CH_3COCl ($\Delta[CH_3COCl]/\Delta[CCl_3CH_3]$) was established. The lack of any CH_3COCl product and the tendency of the $COCl_2$ yield to approach zero in the presence of high O_2 concentrations suggest that the formation of CH_3CCl_2 radicals is of negligible importance.

Implications for Atmospheric Chemistry

Following release into the atmosphere, CCl_3CH_3 will react predominantly with hydroxyl radicals. The atmospheric lifetime of CCl_3CH_3 with respect to reaction with OH is 5.7 ± 0.7 years.[37] Reaction with OH gives CCl_3CH_2 which, within 1 μs, will be converted into the corresponding peroxy radical, $CCl_3CH_2O_2$. We have shown here that $CCl_3CH_2O_2$ radicals react rapidly with NO to produce NO_2 and (by inference) CCl_3CH_2O radicals. Using $k_6 \geq 6.1 \times 10^{-12}$ cm^3 molecule^{-1} s^{-1} together with an estimated background tropospheric NO concentration of 2.5×10^8 cm^{-3},[38] the lifetime of $CCl_3CH_2O_2$ radicals with respect to reaction 6 is calculated to be less than 11 min. Reaction 6 is likely to be an important atmospheric loss of $CCl_3CH_2O_2$ radicals. We have shown here that the atmospheric fate of the alkoxy radical generated in reaction 6 is reaction with O_2 to give CCl_3CHO. The subsequent atmospheric chemistry of CCl_3CHO is believed to be dominated by photolysis and reaction with OH radicals. The atmospheric lifetime of CCl_3CHO with respect to reaction with OH is 290 h.[39] The atmospheric lifetime of CCl_3CHO with respect to photolysis is estimated to be of the order of a few hours.[39] The atmospheric degradation of CCl_3CH_3 in the lower atmosphere gives products which are short lived and incapable of transporting significant amounts of chlorine to the stratosphere.

Acknowledgment. We thank Steve Japar (Ford Motor Company) for a critical reading of the manuscript.

References and Notes

(1) Midgley, P. M. Personal communication, 1994.
(2) World Meteorological Organization, Global Ozone Research and Monitoring Project-Report No. 20; Scientific Assessment of Stratospheric Ozone, Appendix: AFEAS Report, 1989; Vol. 2, Chapter 6.
(3) World Meteorological Organization, Global Ozone Research and Monitoring Project-Report No. 25; Scientific Assessment of Stratospheric Ozone Depletion, 1991; Chapter 5.
(4) Nielsen, O. J. Risø-R-480, 1984.
(5) Wallington, T. J.; Ellermann, T.; Nielsen, O. J. *J. Phys. Chem.* **1993**, *97*, 8442.
(6) Wallington, T. J.; Dagaut, P.; Kurylo, M. J. *Chem. Rev.* **1992**, *92*, 667.
(7) Roussel, P. B.; Lightfoot, P. D.; Caralp, F.; Catoire, V.; Lesclaux, R.; Forst, W. *J. Chem. Soc., Faraday Trans.* **1991**, *87*, 2367.
(8) Ellermann, T.; Sehested, J.; Nielsen, O. J.; Pagsberg, P.; Wallington, T. J. *Chem. Phys. Lett.* **1993**, *218*, 287.
(9) Degaut, P.; Wallington, T. J.; Kurylo, M. J. *Int. J. Chem. Kinet.* **1988**, *20*, 815.
(10) Nielsen, O. J.; Gamborg, E.; Sehested, J.; Wallington, T. J.; Hurley, M. D. *J. Phys. Chem.* **1994**, *98*, 9518.
(11) Lightfoot, P. D.; Cox, R. A.; Crowley, J. N.; Destriau, M.; Hayman, G. D.; Jenkin, M. E.; Moortgat, G. K.; Zabel, F. *Atmos. Environ.* **1992**, *26A*, 1805.
(12) Kurylo, M. J.; Ouellette, P. A.; Laufer, A. H. *J. Phys. Chem.* **1986**, *90*, 437.
(13) Sander, S. P.; Watson, R. T. *J. Phys. Chem.* **1981**, *85*, 2960.
(14) Wallington, T. J.; Ellermann, T.; Nielsen, O. J. *Res. Chem. Intermed.* **1994**, *20*, 265.
(15) Sehested, J.; Ellermann, T.; Nielsen, O. J.; Wallington, T. J.; Hurley, M. D. *Int. J. Chem. Kinet.* **1993**, *25*, 701.
(16) DeMore, W. B.; Sander, S. P.; Golden, D. M.; Hampson, R. F.; Kurylo, M. J.; Howard, C. J.; Ravishankara, A. R.; Kolb, C. E.; Molina, M. J. Jet Propulsion Laboratory Publication 92-20, Pasadena, CA, 1992.
(17) Scollard, D. J. P. Ph.D. Thesis, Chemistry Department, University College Dublin, 1992.
(18) Okabe, H. *Photochemistry of Small Molecules*; John Wiley: New York, 1978.
(19) Wallington, T. J.; Nielsen, O. J. *Chem. Phys. Lett.* **1991**, *187*, 33.
(20) Sehested, J.; Nielsen, O. J.; Wallington, T. J. *Chem. Phys. Lett.* **1993**, *213*, 457.
(21) Wallington, T. J.; Ellermann, T.; Nielsen, O. J.; Sehested, J. *J. Phys. Chem.* **1994**, *98*, 2346.
(22) Sehested, J.; Nielsen, O. J. *Chem. Phys. Lett.* **1993**, *206*, 369.
(23) Sehested, J.; Nielsen, O. J. *Chem. Phys. Lett.* **1993**, *213*, 433.
(24) Wallington, T. J.; Hurley, M. D. *Chem. Phys. Lett.* **1992**, *189*, 437.
(25) Wine, P. H.; Semmes, D. H. *J. Phys. Chem.* **1983**, *87*, 3572.
(26) Wine, P. H.; Semmes, D. M.; Ravishankara, A. R. *Chem. Phys. Lett.* **1982**, *90*, 128.
(27) Tschuikow-Roux, E.; Niedzielski, J.; Faraji, F. *Can. J. Chem.* **1984**, *63*, 1093.
(28) Scollard, D. J.; Treacy, J. J.; Sidebottom, H. W.; Balestra-Garcia, C.; Laverdet, G.; LeBras, G.; MacLeod, H.; Téton, S. *J. Phys. Chem.* **1993**, *97*, 4683.
(29) Tyndall, G. S.; Wallington, T. J.; Hurley, M. D.; Schneider, W. F. *J. Phys. Chem.* **1993**, *97*, 1576.
(30) Lesclaux, R.; Dognon, A. M.; Caralp, F. *J. Photochem. Photobiol., A: Chem.* **1987**, *41*, 1.
(31) Zabel, F.; Kirchner, F.; Becker, K. H. *Int. J. Chem. Kinet.* **1994**, *26*, 827.
(32) Jenkin, M. E.; Hayman, G. D.; Wallington, T. J.; Hurley, M. D.; Ball, J. C.; Nielsen, O. J.; Ellermann, T. *J. Phys. Chem.* **1993**, *97*, 11712.
(33) Nelson, L.; Shanahan, I.; Sidebottom, H. W.; Treacy, J.; Nielsen, O. J. *Int. J. Chem. Kinet.* **1990**, *22*, 577.
(34) Braun, W.; Herron, J. T.; Kahaner, D. K. *Int. J. Chem. Kinet.* **1988**, *20*, 51.
(35) U.S. Standard Atmosphere, 1976; NOAA, NASA, USAF: Washington, DC, 1976.
(36) Wallington, T. J.; Hurley, M. D.; Ball, J. C.; Kaiser, E. W. *Environ. Sci. Tech.* **1992**, *26*, 1318.
(37) Derwent, R. G.; Volz-Thomas, A.; Prather, M. J. World Meteorological Organization Global Ozone Research and Monitoring Project, Report No. 20; Scientific Assessment of Stratospheric Ozone, 1989; Vol. 2, p 124.
(38) Atkinson, R. World Meteorological Organization Global Ozone Research and Monitoring Project, Report No. 20; Scientific Assessment of Stratospheric Ozone, 1989; Vol. 2, p 167.
(39) Barry, J.; Scollard, D. J.; Treacy, J. J.; Sidebottom, H. W. G.; LeBras, G.; MacLeod, H.; Téton, S.; Poulet, G.; Teton, S.; Chichinin, A.; Canosa-Mas, C. E.; Kinnison, D. J.; Wayne, R. P.; Nielsen, O. J. *Chem. Phys. Lett.* **1994**, *221*, 353–358.

JP942872R